

A General Sensing-assisted Channel Estimation Framework in Distributed MIMO Network

Hui Zhou *Member, IEEE*, Xiaolan Liu *Member, IEEE*, Sangarapillai Lambotharan *Senior Member, IEEE*,

Abstract—Joint sensing and communication (JSC) research direction has been envisioned to be a key technology in 6G communications, which has the potential to equip the traditional base station with sensing capability by fully exploiting the existing wireless communication infrastructures. To further enhance wireless communication performance in JSC, sensing-assisted communication has attracted attention from both industry and academia. However, most existing papers focused on sensing-assisted communication under line-of-sight (LoS) scenarios due to sensing limitations, where the sensing target and communication user remain the same. In this paper, we propose a general sensing-assisted channel estimation framework, where the channel estimation accuracy for both LoS and non-line-of-sight (NLoS) are considered. Simulation results demonstrate that our proposed sensing-assisted communication framework achieves higher channel estimation accuracy and throughput compared to the traditional least-square (LS) estimation. More importantly, the feasibility of the proposed framework has been validated to solve the complex channel estimation challenge in distributed multiple input and multiple output (MIMO) network.

Index Terms—Distributed MIMO, Channel estimation, Ray tracing, Sensing-aided communication.

I. INTRODUCTION

The Joint sensing and communication (JSC) system has been recognized as a key technology to support various emerging scenarios in 6G networks, e.g., autonomous driving, digital twin, and extended reality. It enables sensing and communication to efficiently share the hardware and wireless resources in the existing communication infrastructure [1], [2]. Shifted from transmission waveform design, multiple input and multiple output (MIMO) beamforming optimization, and joint resource allocation optimization in single JSC access point (AP) scenario, the more advanced distributed JSC MIMO scenario has received more attention recently, where multiple JSC APs are operating in the same frequency band, and time to achieve higher sensing accuracy and communication performance [2], [3]. Prior work on JSC can be mainly categorized into: 1) *sensing-assisted communication* including sensing-assisted beam tracking/training [4], [5], resource allocation and channel estimation [6]; 2) *communication-assisted sensing* consisting of distributed/networked sensing [7], and channel state information (CSI)-enhanced sensing [8]; and 3) *joint sensing and communication* including waveform design [7], and beamforming optimization [2].

Hui Zhou is with Centre for Future Transport and Cities, Coventry University, U.K. (email:hui.zhou@coventry.ac.uk).

Xiaolan Liu is with School of Electrical, Electronic and Mechanical Engineering, University of Bristol, U.K. (email:xiaolan.liu@bristol.ac.uk).

Sangarapillai Lambotharan is with Institute for Digital Technologies, Loughborough University, U.K. (email:S.Lambotharan@lboro.ac.uk).

In existing sensing-assisted communication works, the authors mainly focused on the line-of-sight (LoS) communication scenario with a single JSC AP, where the sensing target (ST) and the communication user equipment (UE) are assumed to be the same object. In [6], a MIMO radar is first deployed to measure the azimuth information of moving vehicles, and then a gain estimator is developed for channel estimation based on the prior angle information. Although a reflection model for mmWave propagation is presented for environment perception, and the non-line-of-sight (NLoS) mmWave channel can be estimated based on the information of the located reflectors [9]. The authors focused on the static sensing target with a single JSC AP. How to achieve the sensing-assisted NLoS channel estimation in a dynamic wireless environment remains to be solved, especially for distributed MIMO networks.

Motivated by the above challenge, in this paper, we consider a distributed MIMO network where the moving ST causes varying NLoS channel conditions between the APs and UEs. Due to the importance of channel estimation in the distributed MIMO network, we focus on improving the channel estimation accuracy between the APs and the UEs with the obtained prior sensing information of the STs. Specifically, we assume one sensing slot will be introduced for APs to perform sensing capability in each transmission frame in future 6G communications [10]. The proposed sensing-assisted channel estimation algorithm can address the channel estimation challenge in a dynamic wireless environment by using the ray tracing method to calculate both the LoS and NLoS propagation paths. The main contributions are stated as

- Different from existing works that mainly focus on LoS scenarios with a single JSC AP, we proposed a general sensing-assisted channel estimation framework for the distributed MIMO network, which captures the characteristics of both the LoS path and NLoS path via ray tracing;
- It is noted that the proposed sensing-assisted channel estimation framework works in a dynamic environment instead of a static environment, which achieves higher throughput under various target speeds compared to the traditional least-square (LS) channel estimation algorithm.

The rest of the papers are organized as follows. Section II presents the system model and problem formulation. Section III provides the detail of the sensing-assisted channel estimation framework. Section IV illustrates the simulation results. Finally, Section V concludes the paper.

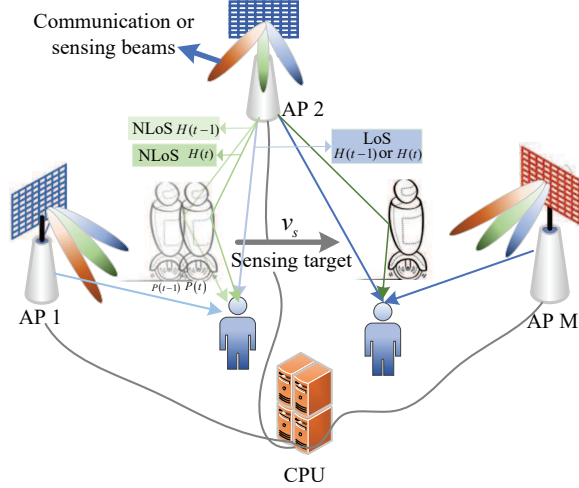


Fig. 1. System model

II. SYSTEM MODEL AND PROBLEM FORMULATION

We consider a distributed massive MIMO JSC system with M access points (APs), where each AP $m \in \mathcal{M} = \{1, \dots, M\}$ is equipped with N_t transmitting antennas and N_r receiving antennas in full-duplex mode. All the APs are connected to a central processing unit (CPU) that can jointly perform design and data processing. We assume there are U UEs, where each UE $u \in \mathcal{U} = \{1, \dots, U\}$ has N_u antennas, and one mobile ST s moving with a speed of v_s on the pre-defined trajectory. It is noted that the ST is modeled as an extended target, whose length l_s and width w_s are assumed to be prior information. As shown in Fig. 1, in the sensing slot, M APs operate in the monostatic radar mode, where each AP m transmits the sensing signal and receives the reflections/scattering from the ST based on full-duplex mode. In the communication slot, all M APs serve the U UEs simultaneously [10].

A. Sensing Signal Model

We consider each AP to be equipped with a uniform linear array (ULA) [11], and transmit the signal towards the center of the ST. We assume the K resolvable scatterers are uniformly distributed in the ST geometry. Hence, once the coordinates of these scatterers are localized, the coordinates of centroid can be uniquely determined. In the n^{th} sensing slot, the received sensing signal at the m^{th} AP can be represented as

$$\mathbf{r}_m^n(t) = \kappa \sqrt{p_m} \sum_{k=1}^K \beta_{m,k}^n e^{j2\pi\mu_{m,k}^n t} \dots \mathbf{b}(\theta_{m,k}^n) \mathbf{a}^H(\theta_{m,k}^n) \mathbf{f}_n s(t - \tau_{m,k}^n) + \mathbf{z}(t), \quad (1)$$

where $\kappa = \sqrt{N_t N_r}$ is the array gain, p_m is the transmit power, $\beta_{m,k}^n$, $\mu_{m,k}^n$ and $\tau_{m,k}^n$ represent the complex reflection coefficient, Doppler frequency, and round-trip delay of k^{th} scatterer. The $\mathbf{b}(\theta)$ and $\mathbf{a}(\theta)$ represent the receive and transmit steering vector, respectively. The $s(t)$ is the transmitted sensing signal, and $\mathbf{z}(t)$ is the additive white Gaussian noise with zero mean and variance of σ^2 , i.e., $\mathbf{z}(t) \sim \mathcal{CN}(\mathbf{0}_{N_r}, \sigma^2 \mathbf{I}_{N_r \times 1})$.

It is noted that the transmit steering vector $\mathbf{a}(\theta)$ and receive steering vector $\mathbf{b}(\theta)$ are presented as follows:

$$\mathbf{a}(\theta) = \frac{1}{\sqrt{N_t}} [1, e^{-j\pi \cos(\theta)}, \dots, e^{-j\pi(N_t-1) \cos(\theta)}]^T, \quad (2)$$

and

$$\mathbf{b}(\theta) = \frac{1}{\sqrt{N_r}} [1, e^{-j\pi \cos(\theta)}, \dots, e^{-j\pi(N_r-1) \cos(\theta)}]^T. \quad (3)$$

where θ represents the AOD and AOA, respectively.

The \mathbf{f}_n represents the beamforming vector, which is written as:

$$\mathbf{f}_n = \mathbf{a}(\hat{\phi}_{n|n-1}^m), \quad (4)$$

where $\hat{\phi}_{n|n-1}^m$ represents the predicted angle of the center of ST based on the $(n-1)^{\text{th}}$ sensing slot measurement.

B. Sensing Measurement Model

We consider the classic radar processing technique, i.e., matched-filtering, to estimate the round-trip delay and Doppler frequency of the scatters. Therefore, the processed signal can be represented as:

$$\begin{aligned} \tilde{\mathbf{r}}_m^n &= \kappa \sqrt{p_m} \sum_{k=1}^K \beta_{m,k}^n \mathbf{b}(\theta_{m,k}^n) \mathbf{a}^H(\theta_{m,k}^n) \mathbf{a}(\hat{\phi}_{n|n-1}^m) \\ &\quad \times \int_0^{\Delta T} s(t - \tau_{m,k}^n) s^*(t - \tau) e^{-j2\pi(\mu - \mu_{m,k}^n)t} dt + \tilde{\mathbf{z}}_r \\ &= \kappa \sqrt{p_m} \sqrt{G} \sum_{k=1}^K \beta_{m,k}^n \mathbf{b}(\theta_{m,k}^n) \mathbf{a}^H(\theta_{m,k}^n) \mathbf{a}(\hat{\phi}_{n|n-1}^m) \\ &\quad \times \bar{\delta}(\tau - \tau_{m,k}^n; \mu - \mu_{m,k}^n) + \tilde{\mathbf{z}}, \end{aligned} \quad (5)$$

where ΔT is the length of the sensing slot, and G represents the matched-filtering gain. The $\bar{\delta}(\tau; \mu)$ represents the normalized matched-filtering output function, which has a narrow mainlobe property in delay domain and Doppler domain to ensure high resolution, i.e., $\bar{\delta}(\tau; \mu) = 1$ when $\tau = 0$, and $\mu = 0$.

Therefore, the measured round-trip delay and Doppler frequency can be represented as:

$$\hat{\tau}_{m,k}^n = \frac{2d_{m,k}^n}{c} + z_{\tau_{m,k}^n}, \quad \hat{\mu}_{m,k}^n = \frac{2v_s \cos(\theta_{m,k}^n) f_c}{c} + z_{\mu_{m,k}^n}. \quad (6)$$

The $\theta_{m,k}^n$ can be measured by the multiple signal classification (MUSIC) algorithm, whose measurements are expressed as

$$\hat{\theta}_{m,k}^n = \theta_{m,k}^n + z_{\theta_{m,k}^n}, \quad (7)$$

where the $z_{\tau_{m,k}^n}$, $z_{\mu_{m,k}^n}$ and $z_{\theta_{m,k}^n}$ are additive noises with zero means and variances of σ_τ^2 , σ_μ^2 , and σ_θ^2 . It is noted that m, n, k are omitted for simplicity.

Then the σ_τ^2 , σ_μ^2 , and σ_θ^2 can be represented as:

$$\sigma_i^2 = \frac{a_i^2 \sigma^2}{p_m G |\kappa \beta_{m,k}^n|^2 |\varrho_{m,k}^n|^2}, \quad i = \tau, \mu, \theta, \quad (8)$$

where $\varrho_{m,k}^n = \mathbf{a}^H(\theta_{m,k}^n) \mathbf{a}(\hat{\phi}_{n|n-1}^m)$ represents the beamforming gain, and a_i are constants related to the system configuration, signal designs, and algorithms.

Finally, we can obtain the measurements of the coordinates of centroid, the angle of the centroid, and the velocity of the ST, which can be represented as

$$\begin{aligned}\hat{x}_n &= \frac{1}{MK} \sum_{m=1}^M \sum_{k=1}^K \hat{c}\hat{\tau}_{m,k}^n \cos \hat{\theta}_{m,k}^n / 2, \\ \hat{y}_n &= \frac{1}{MK} \sum_{m=1}^M \sum_{k=1}^K \hat{c}\hat{\tau}_{m,k}^n \sin \hat{\theta}_{m,k}^n / 2, \\ \hat{v}_n &= \frac{1}{MK} \sum_{m=1}^M \sum_{k=1}^K \frac{\hat{c}\hat{\rho}_{m,k}^n}{2f_c \cos(\hat{\theta}_{m,k}^n)}.\end{aligned}\quad (9)$$

C. Communication Model

We denote the communication channel between UE u and AP m in n^{th} communication slot as $h_{u,m}^n \in \mathbb{C}^{N_u \times N_t}$. Further, by stacking the channels between UE u and all the APs, we construct $h_u^n \in \mathbb{C}^{N_u \times MN_t}$. Next, considering a block fading channel model, where the channel remains constant over the transmission of each slot, we can write the received signal at UE u as

$$\begin{aligned}y_u^n &= \sum_{m \in \mathcal{M}} h_{u,m}^n \mathbf{x}_m + z_u \\ &= \underbrace{\sum_{m \in \mathcal{M}} h_{u,m}^n w_{u,m}^n x_u}_{\text{DesiredSignal}} + \underbrace{\sum_{u' \in \mathcal{U} \setminus \{u\}} \sum_{m \in \mathcal{M}} h_{u,m}^n w_{u',m}^n x_{u'}}_{\text{Interference}} + z_u,\end{aligned}\quad (10)$$

where $w_{u,m}$ represents the beamforming weights of user u at AP m , and z_u is the noise.

D. Problem Formulation

To enhance the channel estimation accuracy, we aim to minimize the mean squared error (MSE) between the ideal channel and the estimated channel, which can be formulated as follows:

$$(\text{OP1}): \quad \min \frac{1}{MU} \sum_{m \in \mathcal{M}} \sum_{u \in \mathcal{U}} \|h_{u,m} - \hat{h}_{u,m}\|_F^2. \quad (11)$$

III. SENSING-ASSISTED MMWAVE CHANNEL ESTIMATION

In this section, the proposed sensing-assisted mmWave channel estimation scheme will be presented. First, assuming one sensing slot is allocated in each transmission frame to detect the position, and velocity of the ST. Then, the obtained sensing information of the ST can be used to calculate the propagation gain between any APs and UEs, by considering both LoS and NLoS propagation paths using the ray tracing method.

A. Multipaths Channel Model

The channel between any AP m and the UE u comprises $L \geq 1$ paths, where assuming the first one is the LoS path, while the others $L - 1$ paths associated with the ST are reflectors or scatters. Here, L satisfies $L \ll \min(N_u, N_m)$ in mmWave propagation, and it has single-bounce reflections.

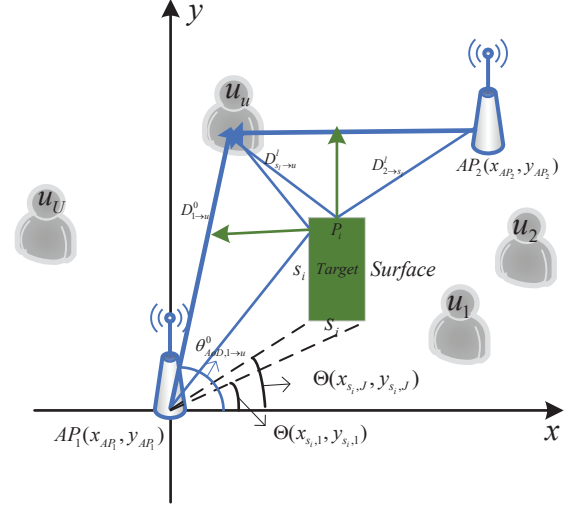


Fig. 2. Propagation reflection model between APs and UEs

Therefore, the channel is considered spatially sparse, and different paths are assumed to be distinct.

Let $\theta_{m,l}$ and $\theta_{u,l}$, $0 \leq l \leq L$, be the DOD and DOA of l^{th} path, respectively. Let $l = 0$ represents the LoS path. Therefore, the channel coefficient between any AP m and the user u can be expressed as

$$H_{m \rightarrow u}(t) = \sum_{l=0}^L I_{m \rightarrow u}^l \sqrt{N_m N_u} \alpha_{m \rightarrow u}^l \mathbf{a}_m^l \mathbf{b}_u^{lH} \quad (12)$$

where $I_{m \rightarrow u}^l = 1$ indicates the propagation path l exists, otherwise not. In the following sections, we will present how to calculate the propagation gain $\alpha_{m \rightarrow u}^l$ under the condition of the LoS path and NLoS path.

B. LoS Path

Since the ST is moving with speed v_s , it causes variations of communication links between UEs and APs, and may lead to NLoS path. Therefore, we have to detect if there are any LoS and NLoS propagation paths. The ST is assumed to be rectangular, if we know the position of the ST, represented with the centroid as (x_s, y_s) , width W_s and length L_s , the four surfaces (i.e., reflective surface) of the ST can be obtained. The four surfaces are represented as $\{s_i, i = 1, 2, 3, 4\}$.

Here, the LoS paths between APs and UE exist only if the ST is not blocking the communication link, i.e., they are not blocked by any surface of the ST, like the LoS link between AP AP_1 and UE u_u shown in Fig. 2. From Fig. 2, each surface can induce an angular range defined as

$$\Omega_{s_i} = \begin{cases} [\Theta(x_{s_i,1}, y_{s_i,1}), \Theta(x_{s_i,J}, y_{s_i,J})], \\ \Theta(x_{s_i,1}, y_{s_i,1}) < \Theta(x_{s_i,J}, y_{s_i,J}) \\ [\Theta(x_{s_i,1}, y_{s_i,1}), 2\pi) \cup [0, \Theta(x_{s_i,J}, y_{s_i,J})], \\ \Theta(x_{s_i,1}, y_{s_i,1}) > \Theta(x_{s_i,J}, y_{s_i,J}). \end{cases} \quad (13)$$

where $\Theta(x_{s_i,1}, y_{s_i,1}), \Theta(x_{s_i,J}, y_{s_i,J})$ are the angles of the two endpoints of the surface s_i . The calculation of $\Theta(x, y)$ can be found in [12].

$$\begin{aligned}
\alpha_{m \rightarrow u}^l &= e^{-j(\hat{\Phi}_{s_i}^l - \frac{2\pi(D_{m \rightarrow s_i}^l + D_{s_i \rightarrow u}^l)}{\lambda})} \\
&\times \sqrt{\eta \left(\min \left(\frac{A_u^l}{W(\theta_{AoD, m \rightarrow u}^l, N_T)(D_{m \rightarrow s_i}^l + D_{s_i \rightarrow u}^l)}, 1 \right) \hat{R}_s^l + \frac{\sin^2(\Theta(\frac{1}{a_l}, 1) - \Theta(x_{m \rightarrow u}^l, y_{m \rightarrow u}^l)) A_u^l}{\sqrt{4(D_{s_i \rightarrow u}^l)^2 + A_u^l{}^2}} \hat{R}_d^l \right)} \\
D_{m \rightarrow s_i}^l &= \sqrt{(x_{s_i}^l - x_m)^2 + (y_{s_i}^l - y_m)^2}, \quad D_{s_i \rightarrow u}^l = \sqrt{(x_{s_i}^l - x_u)^2 + (y_{s_i}^l - y_u)^2}
\end{aligned} \tag{15}$$

Therefore, the LoS paths exist, i.e., $I_{m \rightarrow u}^0 = 1$, if and only if $\Theta(x_u, y_u)$ does not fall within any range Ω_{s_i} , $i = \{1, 2, 3, 4\}$. Then, the corresponding propagation gain of the LoS path $\alpha_l = \alpha_{m \rightarrow u}^0$ is given by [12]

$$\begin{aligned}
\alpha_{m \rightarrow u}^0 &= e^{j\frac{2\pi D_{m \rightarrow u}^0}{\lambda}} \sqrt{\min \left(\frac{A_u^0}{W(\theta_{AoA, m \rightarrow u}^0, N_T) D_{m \rightarrow u}^0}, 1 \right)} \\
D_{m \rightarrow u}^0 &= \sqrt{(x_u - x_m)^2 + (y_u - y_m)^2}
\end{aligned} \tag{14}$$

where A_u^0 is the effective user aperture $A_u^0 = \lambda + (N_u - 1)\lambda |\sin(\theta_{AoA, m \rightarrow u}^0)|$, $D_{m \rightarrow u}^0$ is the distance between the AP m and the user u . $\theta_{AoA, m \rightarrow u}^0, \theta_{AoD, m \rightarrow u}^0$ are the angles of arrival and departure of this path between the AP m and UE u .

C. NLoS Path

Considering the reflective (i.e., NLoS) paths caused by ST, we have to check if there are NLoS paths existing between any AP m and the UE u . The NLoS path exists, i.e., $I_{m \rightarrow u}^l = 1$, if and only if the AP and the mirror UE over the surface s_i have an intersection point, and the reflective path is not blocked by any other surfaces. For instance, in Fig. 2, one NLoS link exists between AP_2 and UE u_u with the reflection point P_i on surface s_i .

Therefore, we can also follow the calculations in [12] to calculate the reflection coefficient (propagation gain) $\alpha_l = \alpha_{m \rightarrow u}^l$ as shown in Equation (15).

In (15), $D_{m \rightarrow s_i}^l$ and $D_{s_i \rightarrow u}^l$ are the distances from the reflection surface s_i to the AP m and the user u , and $\{\hat{\Phi}_{s_i}^l, \hat{R}_s^l, \hat{R}_d^l\}$ denotes the reflection property of the reflective surface. $\hat{\Phi}_{s_i}^l$ is the phase shift determined by the reflection property, $\hat{R}_s^l \in (0, 1)$ and $\hat{R}_d^l \in (0, 1)$ are the specular reflectance and diffuse reflectance of the reflective surface, respectively. $\theta_{AoD, m \rightarrow u}^l, \theta_{AoA, m \rightarrow u}^l$ are the angles of arrival and departure of the NLoS path, and the details of calculation can be found in [12].

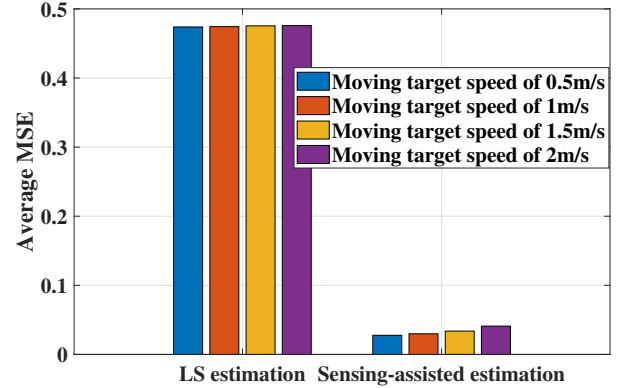
IV. SIMULATION RESULTS

In this section, we evaluate the performance of our proposed sensing-assisted channel estimation method, and the traditional LS channel estimation method is also presented as the benchmark. The indoor scenario is modeled as a 50m square, where the left bottom is the original point, i.e., $O(0, 0)$. Two APs are deployed at $AP_1(0, 0)$ and $AP_2(50, 50)$, respectively. Three UEs are deployed at $u_1(12.5, 37.5)$, $u_2(37.5, 37.5)$, and $u_3(37.5, 25)$, respectively. We assume the moving target ST moves towards the x-axis positive direction with the speed of 1m/s starting from $O_t(0, 12.5)$. It is noted that the length

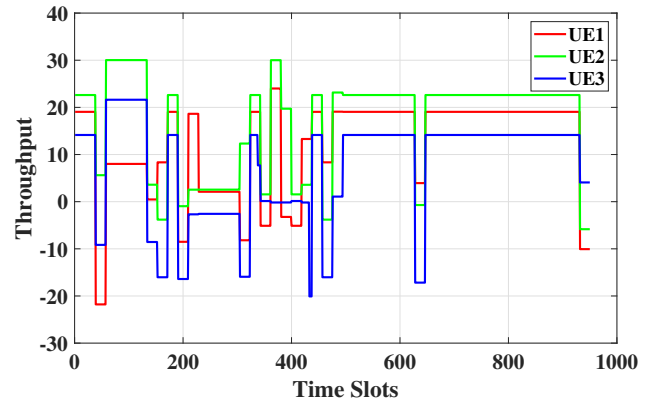
TABLE I
SIMULATION PARAMETERS

| | |
|---|--------------|
| Number of APs M | 2 |
| Number of UEs U | 3 |
| Frequency f_c | 60GHz |
| Transmission power of APs p_m | 23 dBm |
| Number of Transmitting antennas in AP N_t | 128 |
| Number of Receiving antennas in AP N_r | 128 |
| Number of antennas in UE N_u | 4 |
| ST Moving Speed v_s | 1 m/s |
| ST Length l_s | 5 m |
| ST Width w_s | 2 m |
| Number of Scatters K | 10 |
| Noise power σ^2 | -130 dBm |
| a_τ | $3.5e^{-2}$ |
| a_μ | $1.05e^{-2}$ |
| a_θ | $1.05e^{-2}$ |

and width of the moving target are 5m and 2m, respectively. Detailed parameters are given in Table. I.



(a) Average MSE of channel estimation



(b) User throughput gain in different time slots

Fig. 3. Average MSE of channel estimation and user throughput gain in different time slots.

Fig. 3 illustrates the MSE performance of different channel estimation methods and user-level throughput gain over time slots. In Fig. 3 (a), We can observe that the proposed sensing-assisted channel estimation scheme reduces the channel estimation MSE significantly from near 0.5 to around 0.05. Although the MSE of the sensing-assisted scheme increases when the ST is moving with a higher speed, it still achieves much lower MSE than LS estimation. To evaluate the communication performance, we adopt zero-forcing (ZF) beamforming and calculate the corresponding throughput performance. In Fig. 3 (b), We can observe that the proposed sensing-assisted channel estimation scheme achieves higher throughput than the LS estimation in most of the time slots, where sensing error leads to degraded performance in only a few time slots.

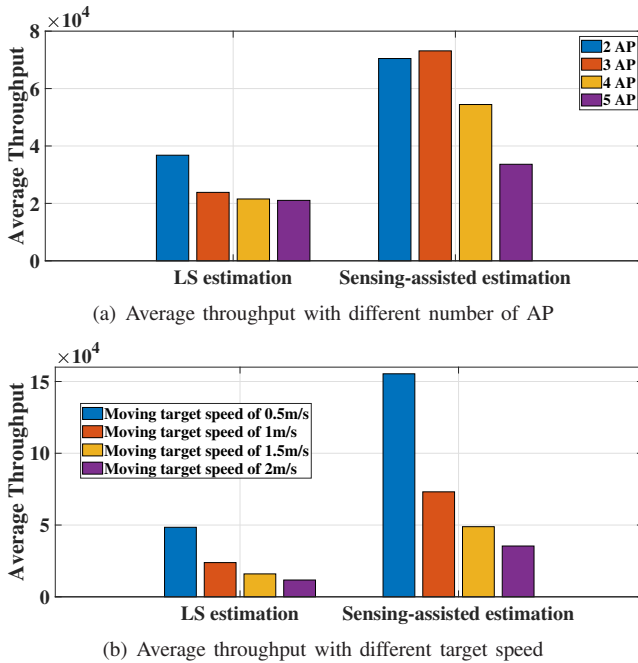


Fig. 4. Average throughput with various number of AP and target speed.

Fig. 4 illustrates the average throughput with different numbers of AP and various moving speeds of the ST. In Fig. 4 (a), We can observe that the average throughput mainly decreases with the increasing number of AP. This is because each AP sacrifices more signal strength to cancel the interference among each other. It is noted that the proposed sensing-assisted scheme achieves a much higher average throughput over different numbers of AP. In Fig. 4 (b), We can observe that the average throughput of both LS estimation and sensing-assisted estimation decreases with increasing the speed of ST.

V. CONCLUSION

In this paper, we proposed a sensing-assisted channel estimation scheme, which exploits the sensing capability of the AP in a distributed MIMO network to enhance channel estimation performance via the ray tracing method. Different from the traditional sensing-assisted communication works focusing on LoS scenarios, the proposed scheme can accurately estimate the NLoS user channel in a dynamic environment caused

by the moving targets, which achieves significant MSE and throughput performance gain compared to the traditional LS estimation.

REFERENCES

- [1] A. Liu, Z. Huang, M. Li, Y. Wan, W. Li, T. X. Han, C. Liu, R. Du, D. K. P. Tan, J. Lu *et al.*, "A survey on fundamental limits of integrated sensing and communication," *IEEE Communications Surveys & Tutorials*, vol. 24, no. 2, pp. 994–1034, 2022.
- [2] U. Demirhan and A. Alkhateeb, "Cell-free isac mimo systems: Joint sensing and communication beamforming," *arXiv preprint arXiv:2301.11328*, 2023.
- [3] Z. Liu, J. Zhang, Z. Liu, H. Du, Z. Wang, D. Niyato, M. Guizani, and B. Ai, "Cell-free xl-mimo meets multi-agent reinforcement learning: Architectures, challenges, and future directions," *arXiv preprint arXiv:2307.02827*, 2023.
- [4] J. Mu, Y. Gong, F. Zhang, Y. Cui, F. Zheng, and X. Jing, "Integrated sensing and communication-enabled predictive beamforming with deep learning in vehicular networks," *IEEE Communications Letters*, vol. 25, pp. 3301–3304, 10 2021.
- [5] L. Cazzella, M. Mizmizi, D. Tagliaferri, D. Badini, M. Matteucci, and U. Spagnolini, "Deep learning-based target-to-user association in integrated sensing and communication systems," 1 2024.
- [6] S. Huang, M. Zhang, Y. Gao, and Z. Feng, "Mimo radar aided mmwave time-varying channel estimation in mu-mimo v2x communications," *IEEE Transactions on Wireless Communications*, vol. 20, pp. 7581–7594, 11 2021.
- [7] F. Liu, Y. Cui, C. Masouros, J. Xu, T. X. Han, Y. C. Eldar, and S. Buzzi, "Integrated sensing and communications: Toward dual-functional wireless networks for 6g and beyond," *IEEE Journal on Selected Areas in Communications*, vol. 40, pp. 1728–1767, 6 2022.
- [8] S. Lu, F. Liu, Y. Li, K. Zhang, H. Huang, J. Zou, X. Li, Y. Dong, F. Dong, J. Zhu, Y. Xiong, W. Yuan, Y. Cui, and L. Hanzo, "Integrated sensing and communications: Recent advances and ten open challenges," *IEEE Internet of Things Journal*, pp. 1–1, 2024.
- [9] C. Jiao, Z. Zhang, C. Zhong, and Z. Feng, "An indoor mmwave joint radar and communication system with active channel perception," in *2018 IEEE International Conference on Communications (ICC)*. IEEE, 2018, pp. 1–6.
- [10] Q. Zhang, H. Sun, X. Gao, X. Wang, and Z. Feng, "Time-division isac enabled connected automated vehicles cooperation algorithm design and performance evaluation," *IEEE Journal on Selected Areas in Communications*, vol. 40, no. 7, pp. 2206–2218, 2022.
- [11] Z. Du, F. Liu, W. Yuan, C. Masouros, Z. Zhang, S. Xia, and G. Caire, "Integrated sensing and communications for v2i networks: Dynamic predictive beamforming for extended vehicle targets," *IEEE Transactions on Wireless Communications*, vol. 22, no. 6, pp. 3612–3627, 2023.
- [12] C. Jiao, Z. Zhang, C. Zhong, X. Chen, and Z. Feng, "Millimeter wave communication with active ambient perception," *IEEE Transactions on Wireless Communications*, vol. 18, no. 5, pp. 2751–2764, 2019.